Scanning Kelvin Probe Microscopy: A Tool to Investigate Nano-Scale Doping Non-Uniformities in Poly-Si/SiO_x Contacts

Preprint

Abhijit S. Kale,[1, 2] Sanjini U. Nanayakkara,[2] William Nemeth,[2] Harvey Guthrey,[2] Matthew Page,[2] Mowafak Al-Jassim,[2] David L. Young,[2] Paul Stradins[2] and Sumit Agarwal[1]

1 Colorado School of Mines
2 National Renewable Energy Laboratory

Presented at the 46th IEEE Photovoltaic Specialists Conference (PVSC 46)
Chicago, Illinois
June 16-21, 2019

NREL is a national laboratory of the U.S. Department of Energy
Office of Energy Efficiency & Renewable Energy
Operated by the Alliance for Sustainable Energy, LLC

This report is available at no cost from the National Renewable Energy Laboratory (NREL) at www.nrel.gov/publications.

Contract No. DE-AC36-08GO28308

Conference Paper
NREL/CP-5900-73161
November 2019

Scanning Kelvin Probe Microscopy: A Tool to Investigate Nano-Scale Doping Non-Uniformities in Poly-Si/SiO_x Contacts

Preprint

Abhijit S. Kale,[1, 2] Sanjini U. Nanayakkara,[2] William Nemeth,[2] Harvey Guthrey,[2] Matthew Page,[2] Mowafak Al-Jassim,[2] David L. Young,[2] Paul Stradins[2] and Sumit Agarwal[1]

Suggested Citation
Kale, Abhijit S., Sanjini U. Nanayakkara, William Nemeth, Harvey Guthrey, Matthew Page, Mowafak Al-Jassim, David L. Young, Paul Stradins and Sumit Agarwal. 2019. *Scanning Kelvin Probe Microscopy: A Tool to Investigate Nano-Scale Doping Non-Uniformities in Poly-Si/SiOx Contacts: Preprint*. Golden, CO: National Renewable Energy Laboratory. NREL/CP-5900-73161. https://www.nrel.gov/docs/fy20osti/73161.pdf.

NREL is a national laboratory of the U.S. Department of Energy
Office of Energy Efficiency & Renewable Energy
Operated by the Alliance for Sustainable Energy, LLC

This report is available at no cost from the National Renewable Energy Laboratory (NREL) at www.nrel.gov/publications.

Contract No. DE-AC36-08GO28308

Conference Paper
NREL/CP-5900-73161
November 2019

National Renewable Energy Laboratory
15013 Denver West Parkway
Golden, CO 80401
303-275-3000 • www.nrel.gov

NOTICE

This work was authored by the National Renewable Energy Laboratory, operated by Alliance for Sustainable Energy, LLC, for the U.S. Department of Energy (DOE) under Contract No. DE-AC36-08GO28308. Funding provided by U.S. Department of Energy Office of Energy Efficiency and Renewable Energy Solar Energy Technologies Office. The views expressed herein do not necessarily represent the views of the DOE or the U.S. Government. The U.S. Government retains and the publisher, by accepting the article for publication, acknowledges that the U.S. Government retains a nonexclusive, paid-up, irrevocable, worldwide license to publish or reproduce the published form of this work, or allow others to do so, for U.S. Government purposes.

Cover Photos by Dennis Schroeder: (clockwise, left to right) NREL 51934, NREL 45897, NREL 42160, NREL 45891, NREL 48097, NREL 46526.

Scanning Kelvin Probe Microscopy: A Tool to Investigate Nano-scale Doping Non-uniformities in *Poly*-Si/SiO_x Contacts

Abhijit S. Kale,[1, 2] Sanjini U. Nanayakkara,[2] William Nemeth,[2] Harvey Guthrey,[2] Matthew Page,[2] Mowafak Al-Jassim,[2] David L. Young,[2] Paul Stradins[2] and Sumit Agarwal[1]

[1]Colorado School of Mines, Golden, CO, 80401, USA, [2]National Renewable Energy Laboratory, Golden, CO, 80401, USA

***Abstract* — We investigate *poly*-Si/SiO_x contacts with both a 1.5 (tunneling-transport) and 2.2 (pinhole-transport) nm SiO_x layer using atomic force microscopy techniques. Conductive AFM on n^+-*poly*-Si/SiO_x/*p*-Si structures show significant spatial variations for both contact types, likely due to non-uniformities in *poly*-Si layer itself. The variations deeper into the contact were revealed by scanning Kelvin probe microscopy after precisely etching away the *poly*-Si/SiO_x layers. The surface potential maps appear similar for both contacts, and show <500 nm size heavily-doped regions. These regions are found to be <200 nm deep for the 2.2 nm contact and >200 nm for the 1.5 nm contact.**

I. Introduction

Exceptionally high efficiencies for crystalline Si (*c*-Si) solar cells (>25%) have been achieved using the *poly*-Si/SiO_x passivated contact approach [1, 2]. Excellent passivation of the *c*-Si surface is obtained using these contacts due to the combined effect of chemical passivation of the SiO_x/*c*-Si interface from the SiO_x layer, and field-effect passivation from the heavily doped *poly*-Si layer. However, optimum contact performance is obtained only when these contacts are annealed at a high temperature: 850 °C for 1.5 nm SiO_x thickness, or >1000 °C for 2.2 nm SiO_x thickness [1, 2]. This high temperature step is required to improve the conductivity through the SiO_x layer by formation of conduction channels, pinholes, as well as to improve the field-effect passivation through dopant diffusion from the *poly*-Si layer, through the SiO_x, into the *c*-Si wafer [3]. Variations in SiO_x layer can affect local conductivity [4] as well as the resultant dopant profiles into *c*-Si, thus affecting local passivation quality. The investigation of these dopant variations using techniques such as secondary ion mass spectrometry is challenging due to the very large area spot size, few microns, resulting in area averaged measurements. Here we, investigate these local doping variations near the *c*-Si surface, and underneath the SiO_x layer, using scanning Kelvin probe microscopy (SKPM), a type of atomic force microscopy (AFM) measurement.

We investigate both tunneling (1.5 nm SiO_x) and pinhole type (2.2 nm SiO_x) *poly*-Si/SiO_x contacts. Conductive AFM (c-AFM) maps on n^+ *poly*-Si/SiO_x/*p*-Si structures show spatial variations in current. The *poly*-Si and SiO_x layers are then precisely etched and the sample surface mapped with SKPM. Heavily doped regions <500 nm in size are mapped in both contacts and their depths estimates by etching the *c*-Si surface.

II. Experimental Details

Double-side polished *p*-Fz *c*-Si, ~1-10 Ω·cm resistivity wafers were cleaned and oxidized in a tube furnace between 700–800 °C in 6:1 N_2:O_2 gas ratios to grow either a ~1.5 or 2.2 nm thick SiO_x layer. For the 1.5 nm SiO_x samples, a phosphorous doped *a*-Si:H layer was deposited on one side using PECVD, and the samples annealed at 850 °C in N_2 to convert *a*-Si:H to *poly*-Si. For the 2.2 nm SiO_x samples, first intrinsic (*i*) *a*-Si:H layer was deposited on one side, and sample annealed at 1025 °C in N_2. Following a treatment with 1% HF, phosphorous doped *a*-Si:H layer was deposited on top of the *i*-*poly*-Si layer, and samples annealed at 850 °C in N_2.

For c-AFM measurements, the samples were treated with 1% HF and then InGa was scratched on the back *p*-Si side. Using Ag-paste, the back side was then adhered to a Cu-tape on a glass slide. The resulting sample (see Fig. 1a) was then immediately loaded in an Ar glove box housing the AFM (Veeco D5000 and NSV controller) system using a Ti/Pt coated Si tip (Asylum Research AC240TM). The contact mode AFM and current images were simultaneously obtained.

For the SKPM measurements, the n^+ *poly*-Si/SiO_x/*p*-Si samples were etched in a control manner using a sequence of 15% tetramethylammonium hydroxide (TMAH) at 80 °C, and

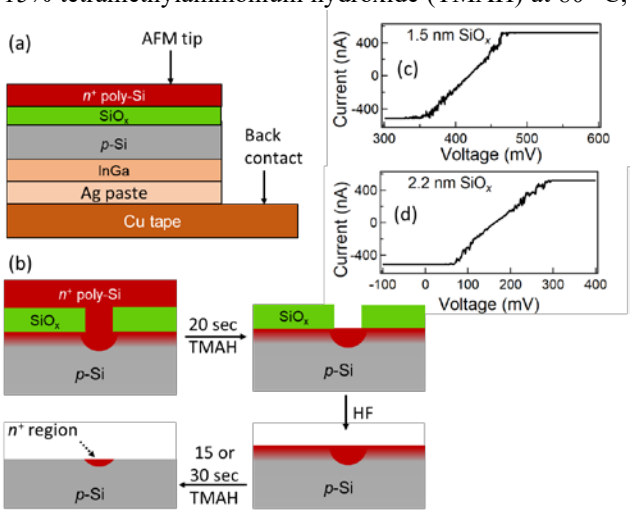

Fig. 1. (a) Schematic of sample stack for c-AFM measurement. (b) Process flow for preparing samples for the SKPM measurement. Current-voltage curves of n^+ *poly*-Si/SiO_x/*p*-Si structures with (c) 1.5 nm SiO_x and (d) 2.2 nm SiO_x layers using c-AFM.

1% HF steps. These have been schematically shown in Fig. 1b. The 2nd TMAH etch was performed for either 15s or 30s. Following a treatment with 1% HF the samples were stacked as previously described for the c-AFM measurements and immediately loaded in the glove box. Surface topography in tapping mode and SKPM measurements were recorded simultaneously in a single-pass mode with an external Kelvin Probe Control Unit (Omicron, Kelvin Probe CU) and an external high-frequency lock-in amplifier (Signal Recovery, 7280 DSP) connected to the AFM using a Pt/Ir coated AFM tip (Nanosensors PPP-EFM).

III. Results and Discussion

A. Investigation of n^+ poly-Si/SiO_x/p-Si structures with c-AFM

Figure 1b and 1c show the J-V curves at a random point measured using the c-AFM setup for the contacts with 1.5 and 2.2 nm SiO_x layers. For both contacts, we saturate our instrument in both forward and reverse bias conditions. While conducting under reverse bias is puzzling, we do verify the presence of a solar cell since the zero-current condition occurs at a non-zero voltage. While further investigation is needed, we currently relate this to a photo-voltage generated due the laser within the AFM instrument or stray light. In order to ensure that we don't saturate our instrument while performing 2D current maps, we measured the 1.5 and 2.2 nm SiO_x contacts under a biasing voltage of 420 and 200 mV, respectively, which is close to their zero-current condition.

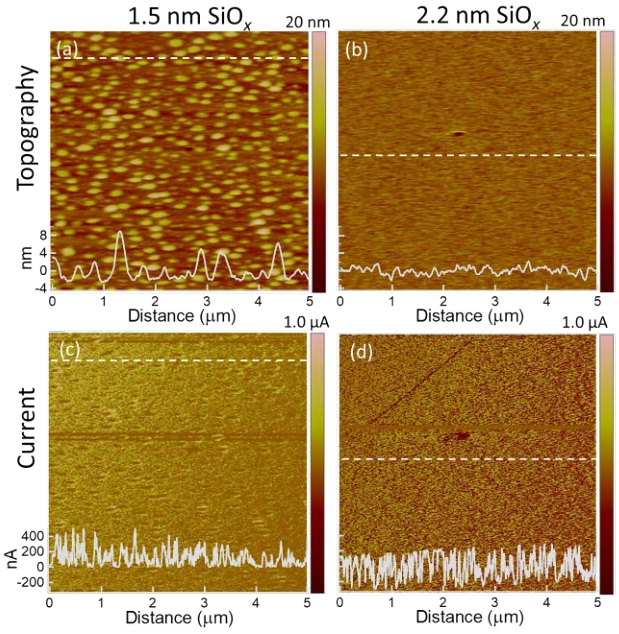

Fig. 2. Topography maps of n^+ *poly*-Si/SiO_x/*p*-Si structures with (a) 1.5 nm SiO_x and (b) 2.2 nm SiO_x layers. (c, d) Corresponding current maps for the images shown in 'a' and 'b'. The inset at bottom of each map shows the line profiles measured across the dashed-line in each map.

The topography maps in Fig. 2a and 2b show that the *poly*-Si film on the 1.5 nm SiO_x contact is rougher than the same on the 2.2 nm SiO_x contact. This could be related to either the different PECVD conditions for phosphorous and intrinsic *a*-S:H films or growth of *a*-Si:H films on SiO_x layers of different thicknesses. The current maps for the same regions (Fig. 2c and 2d) however, show spatial fluctuations in current of 100s of nA over 10s of nm distances. While Zhang et al. [5] have related these fluctuations in current to pinholes in the SiO_x layer, Morisset et al. [6] have related it to variations in the *poly*-Si film. Our similar maps for contacts with both SiO_x thicknesses seem to support the later, i.e., changes in *poly*-Si films such as grains versus grain boundaries might be cause of these current variations. This is further supported by the fact that adjacent pinholes in SiO_x layer are separated by 10s of microns rather than 10s of nm distances when similarly processed samples were analysed using electron beam induced current measurements.

B. *Investigation of spatial doping variations using SKPM*

We investigated the doping variations underneath the SiO_x layer using very selective etch chemistries by removing the n^+ *poly*-Si and SiO_x layers (see Fig. 1b). SKPM is very sensitive to the sample surface and hence, in order to improve the contrast between the n^+ regions formed due to dopant diffusion from *poly*-Si and the *p*-type wafer, we etch a few 100s of nm of the *c*-Si surface. This is expected to remove any near-surface phosphorous doped regions leaving behind only the heavily

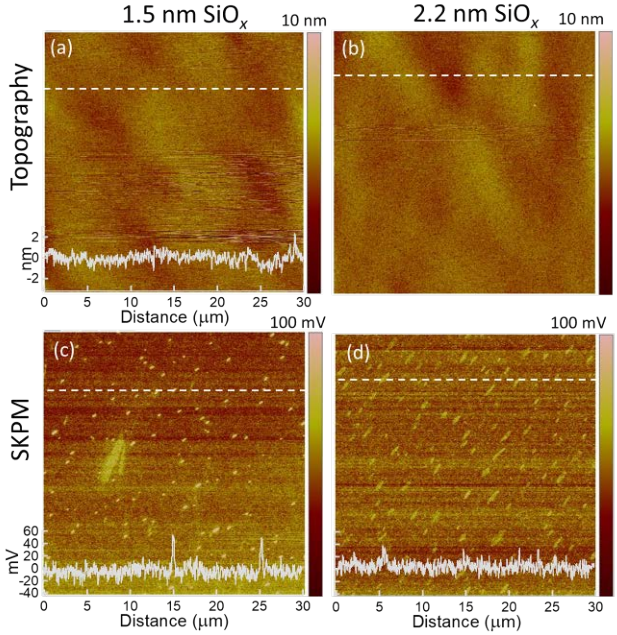

Fig. 3. AFM maps of etched poly-Si contacts using procedure as shown in Fig. 1b, with 2nd TMAH etch performed for 15 sec. (a b) Topography maps of contacts with initial 1.5 and 2.2 nm SiO_x layers, respectively. (c, d) Corresponding SKPM maps for the images shown in 'a' and 'b'. The inset at bottom of each map shows the line profiles measured across the dashed-line in each map.

doped phosphorous regions. We investigated this using two different etching times. The topography maps in Fig. 3a and 3b measured after 15 sec of 2nd TMAH etch (~125 nm of Si etched) of the contacts with 1.5 and 2.2 nm SiO_x layer are flat indicating that our etching is uniform and not introducing any etching artefacts. The SKPM maps for the same (see Fig. 3c and 3d) show regions with <500 nm in size which are more *n*-type than the background. There is no significant difference between the density of these regions between the two contacts. Figure 4 shows similar maps to Fig. 3 but with the 2nd TMAH etch performed for 30 sec (~250 nm of Si etched) instead of 15 sec. Here, while the topography map for 2.2 nm contact is featureless, the same for the 1.5 nm contact shows pits ~15 nm deep and >1 um in size. Similar etch-pits have been observed previously using TMAH [7]. However, the removal of SiO_x prior to performing the 2nd TMAH etch should not result in the formation of such features and these should be observed irrespective of the SiO_x thickness. Interestingly, the SKPM map for the 1.5 nm SiO_x contact (Fig. 4c) does not change significant after the longer etch time. However, for the 2.2 nm SiO_x contact (see Fig. 4d), the density of the heavily doped regions decreases indicating that the longer etch, 30 sec as compared to 15 sec, etches away some of these heavily doped regions. While further investigation of these samples and measurement is needed, the fact that the SKPM features do not directly relate to any topographical features, leads us to conclude that there are indeed some spatial doping non-uniformities underneath the SiO_x layer for both then 1.5 and 2.2 nm SiO_x contacts. These are visible only due to the high sensitivity of the SKPM measurement and the precise etching process performed for these samples.

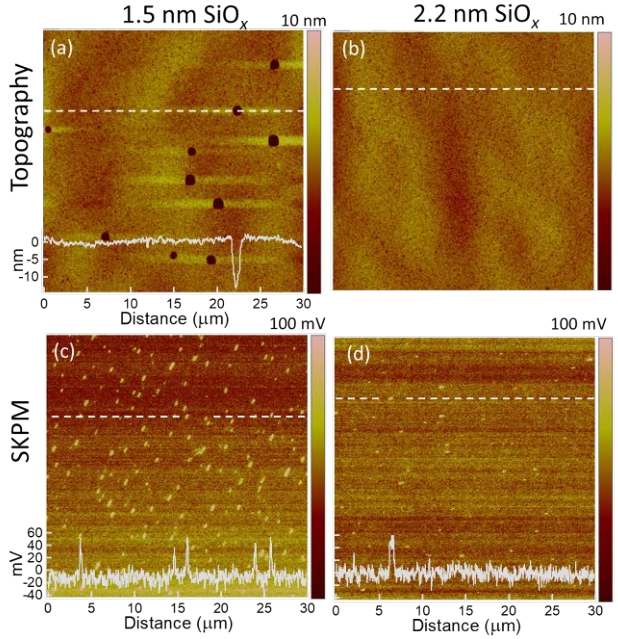

Fig. 4. Same description as Fig, 4 but contacts etched for 30 sec during 2nd TMAH instead of 15 sec.

IV. Conclusions

In summary, we have investigated *poly*-Si/SiO_x contacts using AFM-based characterization techniques: c-AFM and SKPM. 2D c-AFM surface current maps of n^+ *poly*-Si/SiO_x/*p*-Si structures with both 1.5 and 2.2 nm SiO_x thickness show significant spatial fluctuations, likely related to non-uniformities in *poly*-Si conductivity. In order to investigate buried non-uniformities, it is essential to precisely etch away the *poly*-Si and SiO_x layers. SKPM measurements performed after such precise etching shows regions with more *n*-type doping than surrounding regions. The maps are similar for both SiO_x thickness contacts. However, further increasing the etch time significantly reduces the density of these regions for the 2.2 nm SiO_x contact while not affecting the 1.5 nm SiO_x contact, suggesting that these high doping regions have different depths in the two contacts.

Acknowledgements

This work was supported by the U.S. Department of Energy under Contract No. DE-AC36-08GO28308 with Alliance for Sustainable Energy, LLC, the Manager and Operator of the National Renewable Energy Laboratory. Funding provided by U.S. Department of Energy Office of Energy Efficiency and Renewable Energy Solar Energy Technologies Office under Agreement Number 34359. The views expressed in the article do not necessarily represent the views of the DOE or the U.S. Government. The U.S. Government retains and the publisher, by accepting the article for publication, acknowledges that the U.S. Government retains a nonexclusive, paid-up, irrevocable, worldwide license to publish or reproduce the published form of this work, or allow others to do so, for U.S. Government purposes.

References

[1] F. Haase *et al.*, "Interdigitated back contact solar cells with polycrystalline silicon on oxide passivating contacts for both polarities," *Japanese Journal of Applied Physics,* vol. 56, no. 8S2, p. 08MB15, 2017.

[2] A. Richter, J. Benick, F. Feldmann, A. Fell, M. Hermle, and S. W. Glunz, "n-Type Si solar cells with passivating electron contact: Identifying sources for efficiency limitations by wafer thickness and resistivity variation," *Solar Energy Materials and Solar Cells,* vol. 173, pp. 96-105, 2017/12/01/ 2017.

[3] A. S. Kale *et al.*, "Effect of silicon oxide thickness on polysilicon based passivated contacts for high-efficiency crystalline silicon solar cells," *Solar Energy Materials and Solar Cells,* vol. 185, pp. 270-276, 10// 2018.

[4] K. Lancaster, S. Großer, F. Feldmann, V. Naumann, and C. Hagendorf, "Study of Pinhole Conductivity at Passivated Carrier-selected Contacts of Silicon Solar Cells," *Energy Procedia,* vol. 92, pp. 116-121, 2016/08/01/ 2016.

[5] Z. Zhang *et al.*, "Carrier transport through the ultrathin silicon-oxide layer in tunnel oxide passivated contact (TOPCon) c-Si solar cells," *Solar Energy Materials and Solar Cells,* vol. 187, pp. 113-122, 2018/12/01/ 2018.

[6] A. Morisset *et al.*, "Conductivity and Surface Passivation Properties of Boron-Doped Poly-Silicon Passivated Contacts for c-Si Solar Cells," *physica status solidi (a),* vol. 0, no. 0, p. 1800603, 2018/10/05 2018.

[7] A. S. Kale *et al.*, "Tunneling or Pinholes: Understanding the Transport Mechanisms in SiOx Based Passivated Contacts for High-Efficiency Silicon Solar Cells," in *7th World Conference on Photovoltaic Energy Conversion*, Waikoloa, Hawaii, USA, 2018.